Supporting Information

Hou et al. 10.1073/pnas.0907724106

SI Methods

Animal Protocols. All mice were bred and maintained according to the Harvard Medical School animal research requirements, and all procedures were approved by the Institutional Animal Research and Care committee. The generation of CLDN16 KD mice has been described by Hou et al. (1). To generate CLDN19 KD mice, female donor mice (B6D2F1 hybrid strain) were superovulated with a combination of pregnant mare serum (5 units) and human CG (5 units). On average, ≈20–30 embryos were collected per female. Approximately 10 to 100 pL of concentrated lentivirus at 10^6 units/μL were injected into the perivitelline space of single cell mouse embryos and allowed to develop to two-cell embryo stage. Around 20 embryos were implanted into each pseudopregnant female (CD-1 strain; 0.5 dpc) and carried to term. The transgenic founder mice were crossed to WT C57BL/6 mice (Charles River Lab), and progeny were analyzed. Littermate WT mice were used as controls. All mice were fed ad libitum and housed under a 12-h light cycle.

Surgical Protocols and Renal Clearance. The method for performing renal clearance measurements in the mouse has been described in ref. 1. Mice were anesthetized by i.p. injection of Inactin (Sigma; 100 mg/kg). The jugular vein was catheterized for i.v. infusion of PBS at 2 μL/min, with 1% FITC-inulin included in the infusate. After an equilibration period of 60 min, renal clearance measurements were carried out for a 60-min period. Urine was collected under mineral oil, and a 30-μL blood sample was taken at hourly intervals. Urine and plasma Na^+, K^+, Mg^{2+}, and Ca^{2+} concentrations were measured by flame photometry (type 480 Flame Photometer; Corning Medical and Scientific). Mouse serum aldosterone levels were measured by using ELISA (Alpha Diagnostic).

Real-Time Quantitative PCR. Gene expression was quantified by real-time quantitative PCR by using iQ SYBR green supermix (Bio-Rad) and the ABI Prism 7700 Sequence Detection System (Applied Biosystems). Total RNA was extracted from the kidney by using the TRIzol reagent (Invitrogen). The amount of kidney total RNA for each reaction was adjusted within the range 0.05–0.2 μg, depending on the gene, to ensure that gene expression was within the range of linear correlation between the log (amount of total RNA) and threshold cycle number. The housekeeping gene β-actin was used as an endogenous control, and the expression levels of genes of interest were presented as ratios relative to the expression level of β-actin. The primers annealed to two adjacent exons to avoid amplifying genomic DNA and the primer sequences (5′ end to 3′ end) were summarized as follows: CLDN16, CAAACGCTTTTGATGGGATTC and TTTGTGGGTCATCAGGTAGG; CLDN19, CGGGCAGGTGCAATGCAAAC and CAGGAGACAGCAGTCAAAGTA; β-actin, CTGCCTGACGGCCAAGTC and CAAGAAGGAAGGCTGGAAAAGA.

Protein Electrophoresis and Immunoblotting. Both kidneys from each mouse were homogenized by using a Dounce homogenizer in ice-cold water containing 50 mM Tris (pH 8.0), rupturing the membrane of cells. The homogenate was centrifuged in conical tubes at 5,000 × g for 20 min to remove cytosolic proteins. The sediment was resuspended in RIPA buffer [150 mM NaCl, 0.5 mM EDTA, 1% Triton X-100, 0.1% SDS, 50 mM Tris·HCl (pH 8.0)] to extract membrane proteins. Fifty micrograms of membrane proteins were subjected to SDS/PAGE under denaturing conditions and transferred to a nitrocellulose membrane followed by blocking with 3% milk, incubation with primary claudin antibodies (1:1,000) and the horseradish peroxidase-labeled secondary antibody (1:5,000), and exposure to an ECL Hyperfilm (Amersham Biosciences). Molecular mass was determined relative to protein markers (Bio-Rad).

Immunolabeling and Fluorescence Microscopy. For viewing claudin expression and localization in the kidney, fresh cryostat sections (10 μm) were fixed with cold methanol at −20°C, followed by blocking with PBS containing 10% FBS, incubation with primary antibodies (1:300) and FITC or rhodamine-labeled secondary antibodies (1:200). After washing with PBS, slides were mounted with Mowiol (Calbiochem). Images were collected with a Nikon E800 photomicroscope equipped with a SPOT-2 digital camera. The 5-Mb TIFF images were collected and converted to JPEG format and arranged by using Photoshop 6.0 (Adobe).

Y2H Membrane Protein Interaction Assay. The Y2H membrane protein interaction assay (MoBiTec Molecular Biotechnology) for analyzing the specific claudin interactions [CLDN16 (AF152101), CLDN19 (BC030524), CLDN10 (isoform a, BC029019; b, BC021770), and CLDN18 (isoform a1.1, BC142708; a2.1, AF349451)] has been described by Hou et al. (2). The DNA fragments were amplified by using PCR and cloned into the vectors pBT3-C/N such that they were in frame with the Cub-TF cassette placed downstream/upstream, respectively (for "bait vectors" with C-Ubiquitin fusion), and similarly into the vectors pPR3-C/N (for "prey vectors" with N-Ubiquitin fusion). The assay was performed by transforming the yeast strain NMY51 with 1.5 μg of bait vectors. Verification of correct topology of all of the baits was performed by using pAI-Alg5 and pDL2-Alg5 control preys, and the upper limit of selection stringency of the baits was determined by using selective triple drop-out medium lacking leucine, tryptophan, histidine, and adenine (SD-LWHA). The yeast strains expressing the bait proteins were transformed with 1.5 μg of prey vectors. Transformed yeast cells were plated on drop-out media lacking leucine and tryptophan (SD-LW) and incubated for growth of positive transformants. Three to six independent positive transformants were then selected and resuspended in 50 mL of 0.9% NaCl buffer; 5 μL of each suspension was spotted on SD-LWHA media. Growth of colonies on the selective medium was scored as positive for interaction. To further verify the positive interactions, β-galactosidase activity was performed by using a filter lift assay, following the manufacturer's protocols (MoBiTec GmbH). To determine the strength of interaction, quantitative measurements of β-galactosidase activity were performed by lysing the yeast pellets of 1-mL overnight culture, with 0.05 M Tris (pH 8.8), 1% SDS, and ≈100 μL of acid-washed glass beads (Sigma-Aldrich), followed by three freeze–thaw cycles in liquid nitrogen. The lysate was incubated for 30 min with 10 μL of 10% X-Gal (Carl Roth). Color development was measured by using a spectrophotometer and scored as an indicator of the strength of the interaction. Blank measurements were performed with untransformed yeast cells grown in YPAD medium.

Statistical Analyses. The significance of differences between groups was tested by ANOVA (Statistica 6.0, Statsoft 2003). When the all-effects F value was significant ($P < 0.05$), post hoc analysis of differences between individual groups was made with the Newman–Keuls test. Values were expressed as mean ± SE, unless otherwise stated.

1. Hou J, et al. (2007) Transgenic RNAi depletion of claudin-16 and the renal handling of magnesium. *J Biol Chem* 282:17114–17122.

2. Hou J, et al. (2008) Claudin-16 and claudin-19 interact and form a cation-selective tight junction complex. *J Clin Invest* 118:619–628.

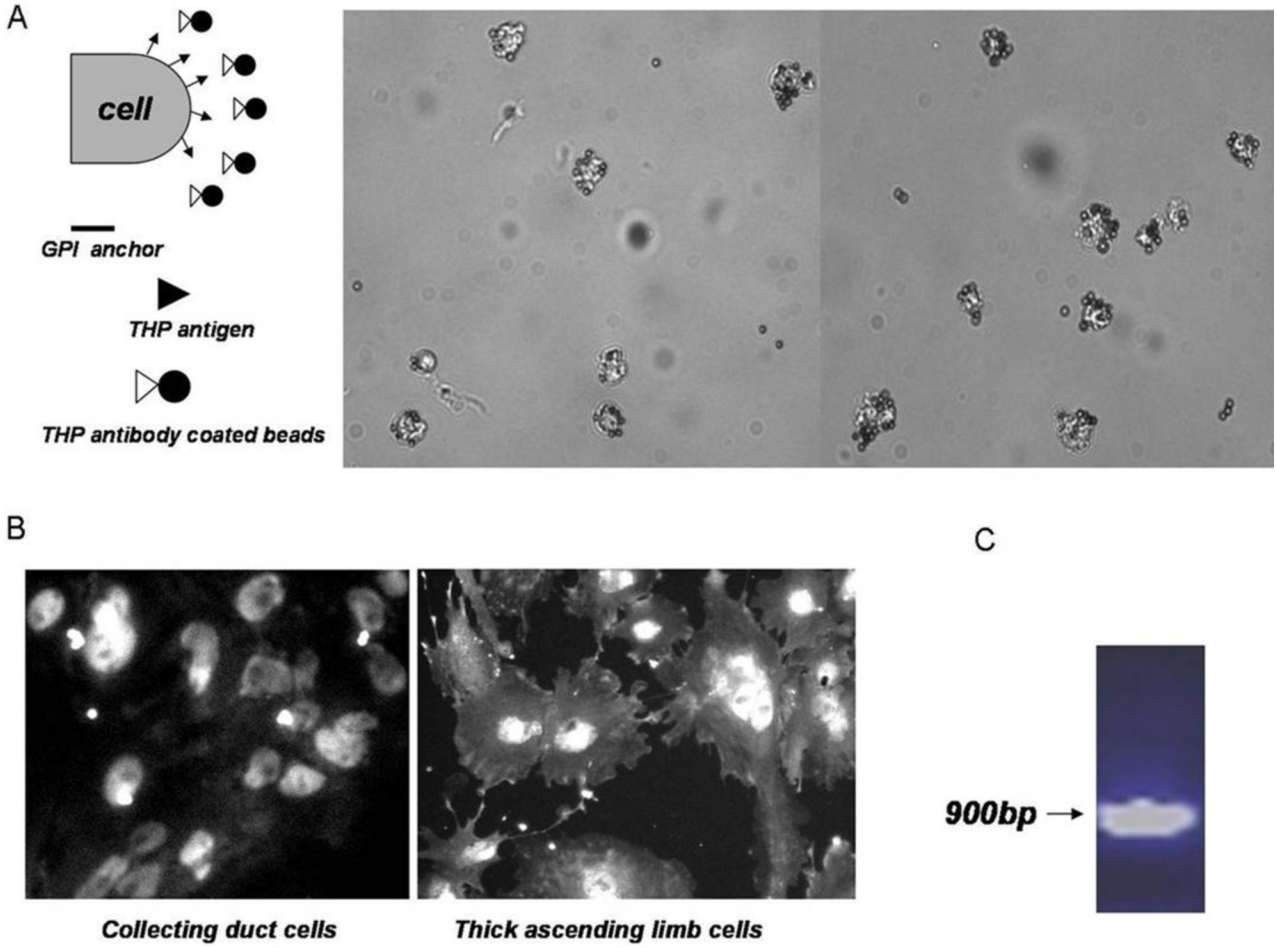

Fig. S1. Immunoisolation of the TAL cells from the mouse kidney. (*A*) Immunoprecipitation of TAL cells by using magnetic beads coated with the THP antibody. (*B*) Immunostaining of isolated TAL cells with the THP antibody (*Right*); compared with cultured collecting duct cells (M-1) as control (*Left*). Note the THP labeling in the plasma membrane of the TAL cells. (*C*) The RT-PCR analysis of isolated TAL cells showing the expression of a TAL-specific gene CLDN16.

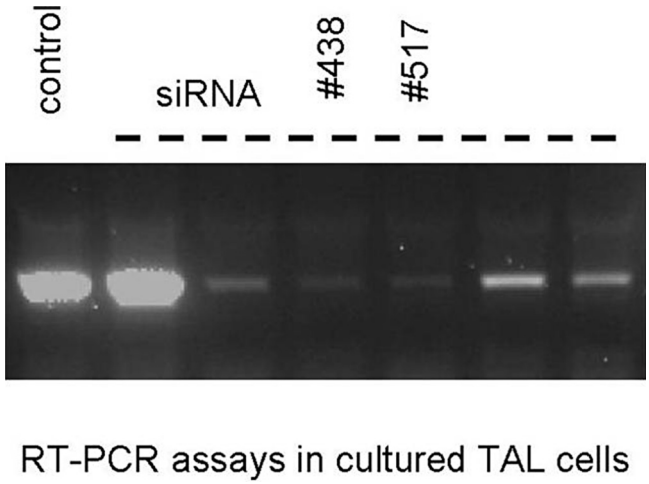

Fig. S2. Determination of siRNA sequences for silencing CLDN19 in cultured mouse TAL cells. Numbers 438 and 517 were selected for development of transgenic mouse lines.

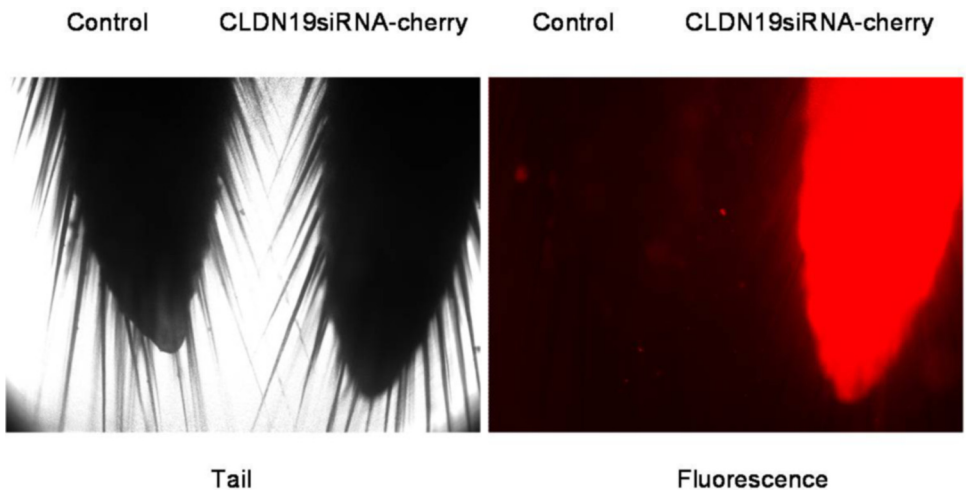

Fig. S3. Transgenic CLDN19 KD pups can be directly genotyped by using the fluorescent protein cherry that is expressed downstream of the ubiquitin promoter.

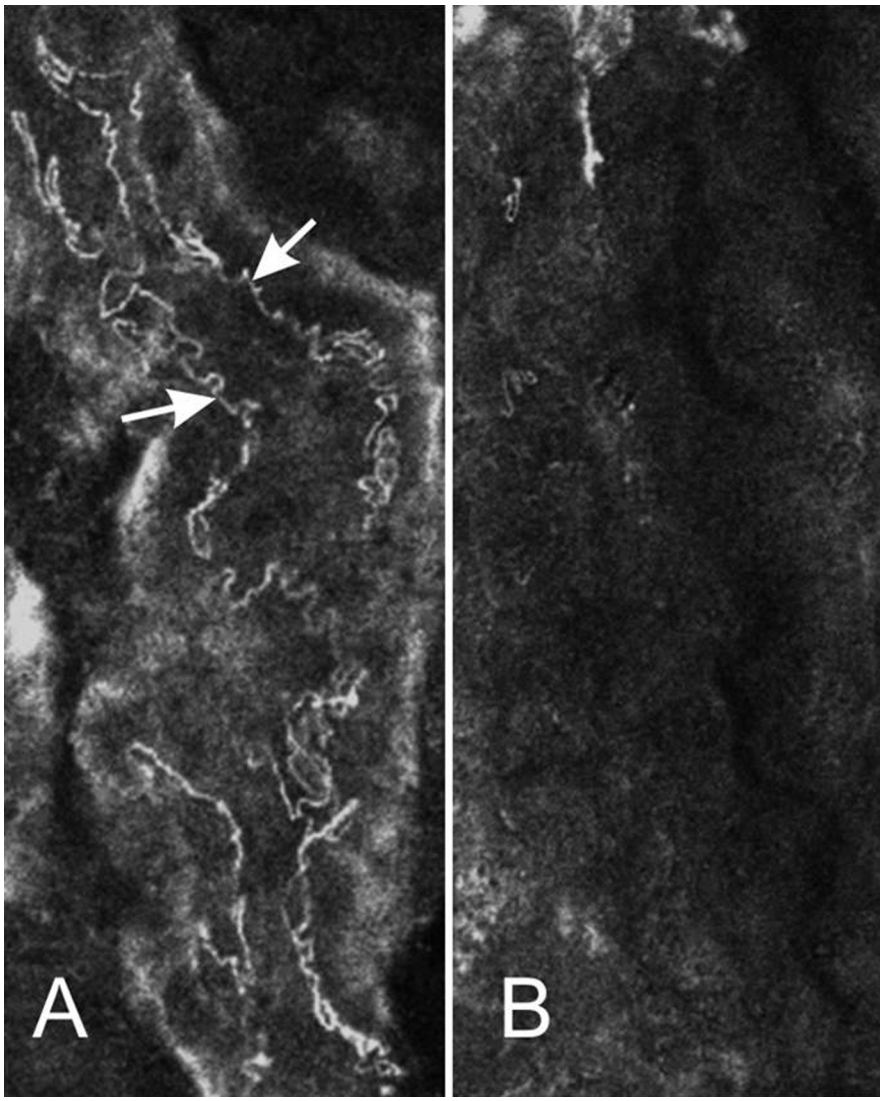

Fig. S4. Immunofluorescence analysis of CLDN19 protein level in the kidney of WT (*A*) and CLDN19 KD (*B*) mouse. TJ staining in the TAL seen at the arrows in *A* is missing in *B*. (Scale bar: 10 μm.)

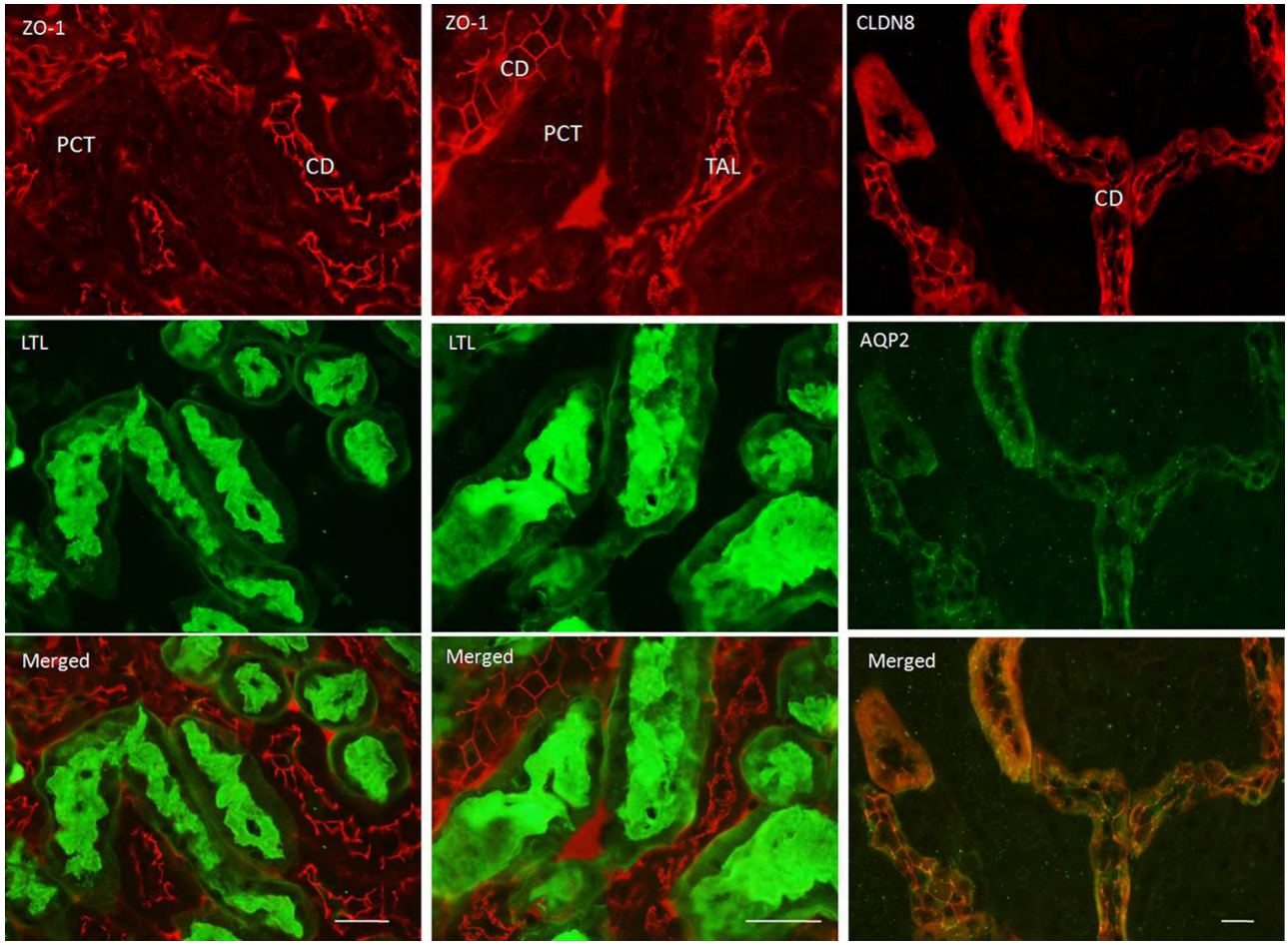

Fig. S5. Immunolocalization of ZO-1 and CLDN8 in the mouse kidney. The *Lotus tetragonolobus* lectin (LTL) selectively labels the brush border of the proximal convoluted tubule (PCT). Aquaporin 2 (AQP2) is a specific marker for the collecting duct (CD). Note TJ strands in PCT and CD are shown as straight lines, but TJ strands in CD have much stronger staining than in PCT, consistent with observations that TJs in the distal nephron are tighter and have more strands and higher transepithelial resistance (TER). The TJ strands in the TAL are seen as interdigitated lines. (Scale bar: 10 μm.)

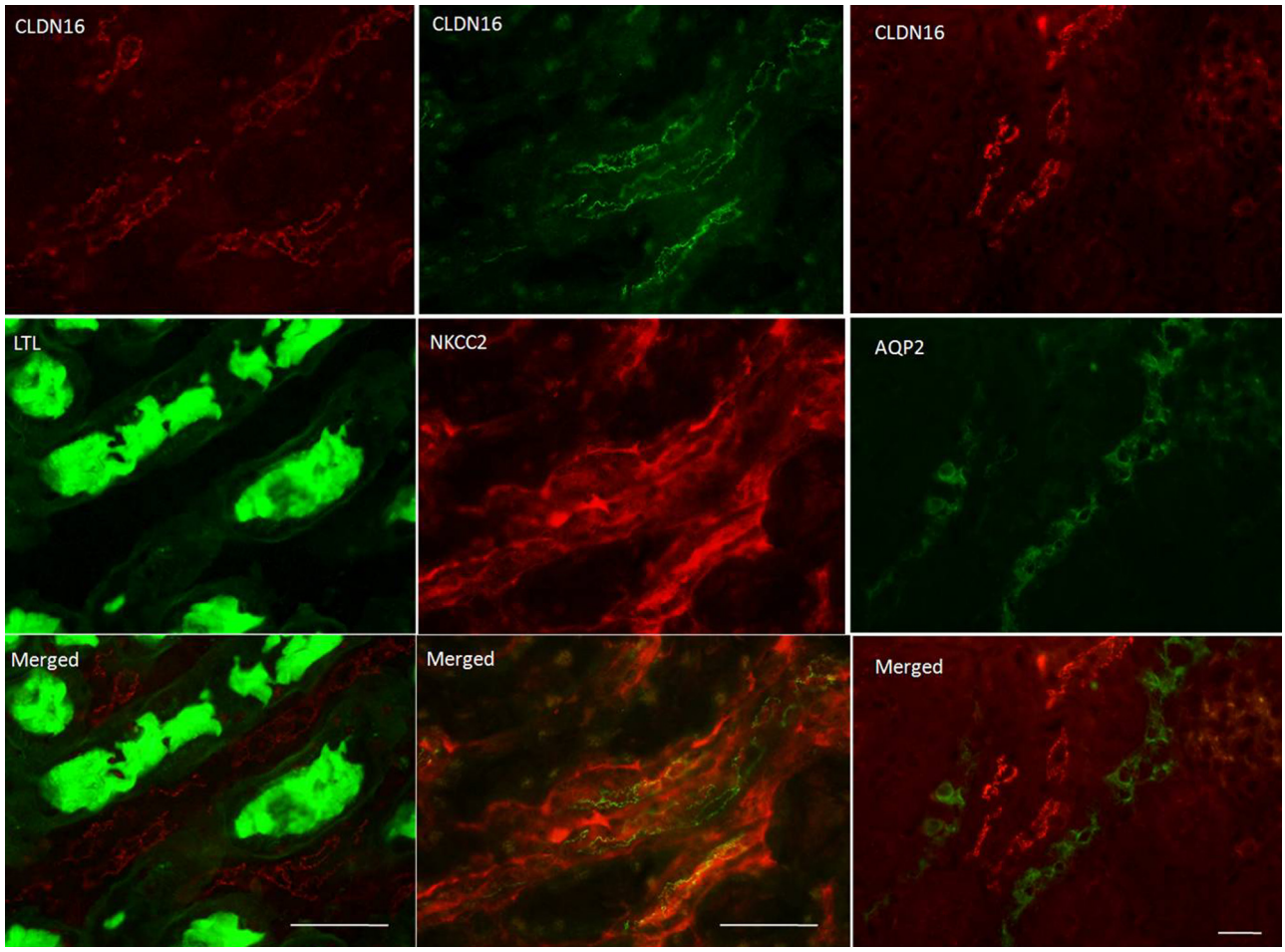

Fig. S6. Immunolocalization of CLDN16 in the TAL of mouse kidney. The *Lotus tetragonolobus* lectin (LTL) selectively labels the brush border of the proximal convoluted tubule (PCT). Na/K/Cl-cotransporter 2 (NKCC2) is a specific marker for the TAL, whereas aquaporin 2 (AQP2) a specific marker for the collecting duct (CD). Note CLDN16 is colocalized with NKCC2 but not with LTL or AQP2. (Scale bar: 10 μm.)

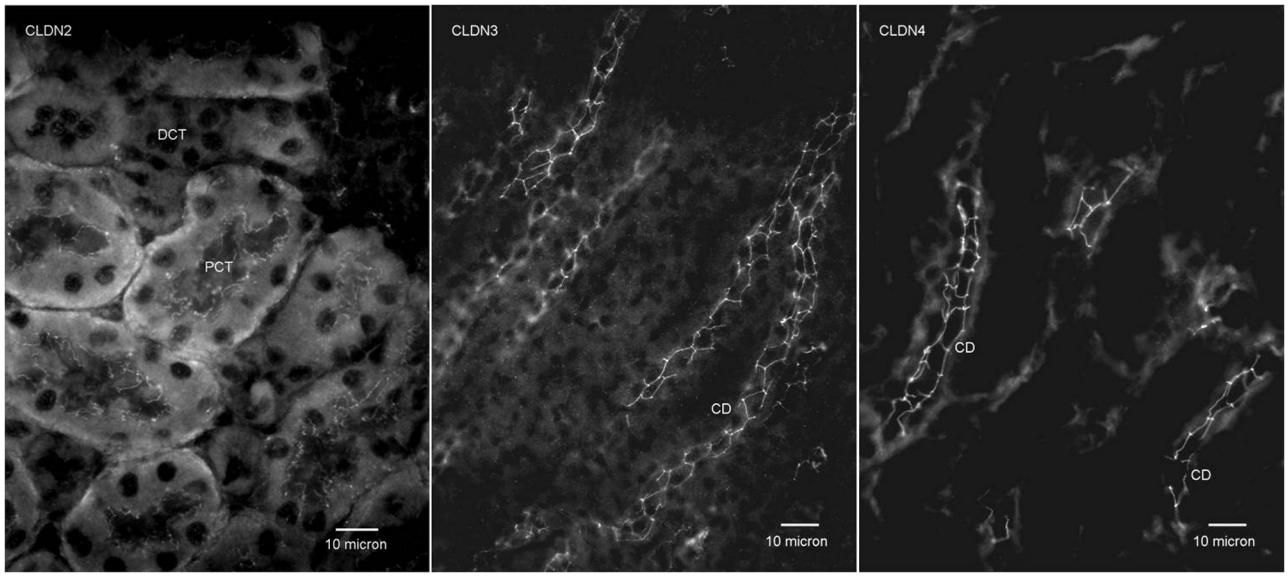

Fig. S7. Immunolocalization of CLDN2, CLDN3, and CLDN4 in mouse kidney, respectively. Note TJ strands in PCT and CD are shown as straight lines, but TJ strands in CD have much stronger staining than in PCT, consistent with observations that TJs in the distal nephron are tighter and have more strands and higher transepithelial resistance (TER). PCT, proximal convoluted tubule; DCT, distal convoluted tubule; CD, collecting duct.

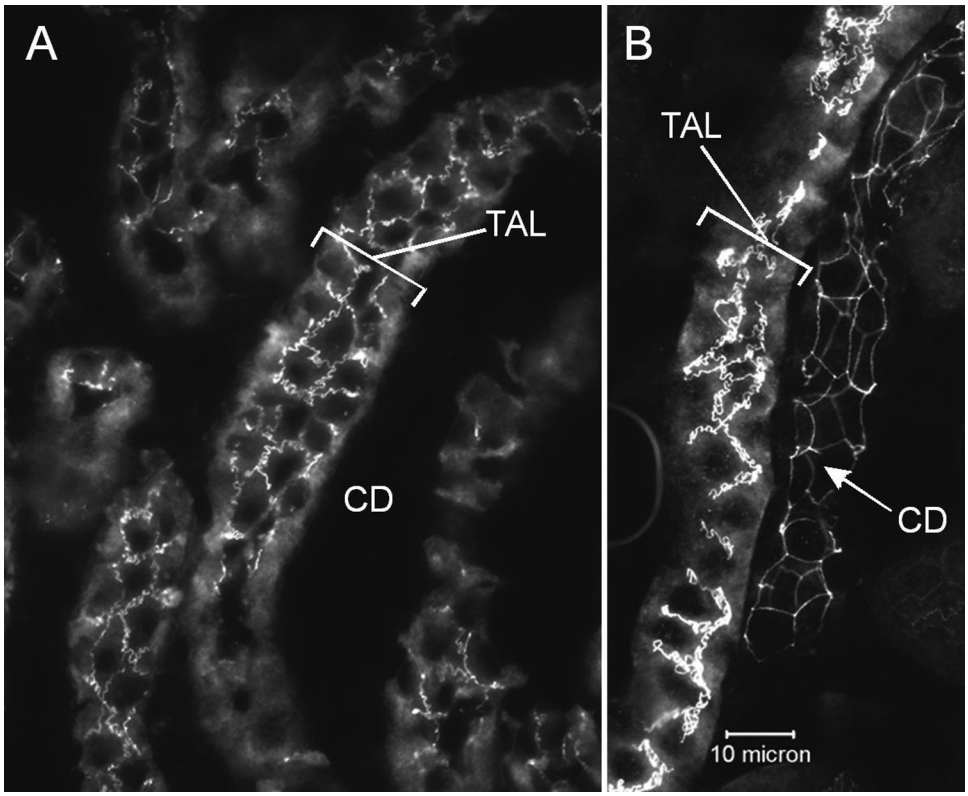

Fig. S8. (*A*) Immunolocalization of CLDN10 in mouse kidney. (*B*) Immunolocalization of CLDN18 in mouse kidney. Note TJ strands in the TAL are shown as interdigitated lines along the apical surface of the tubule, whereas TJ strands in the CD are shown as straight lines. CD, collecting duct.

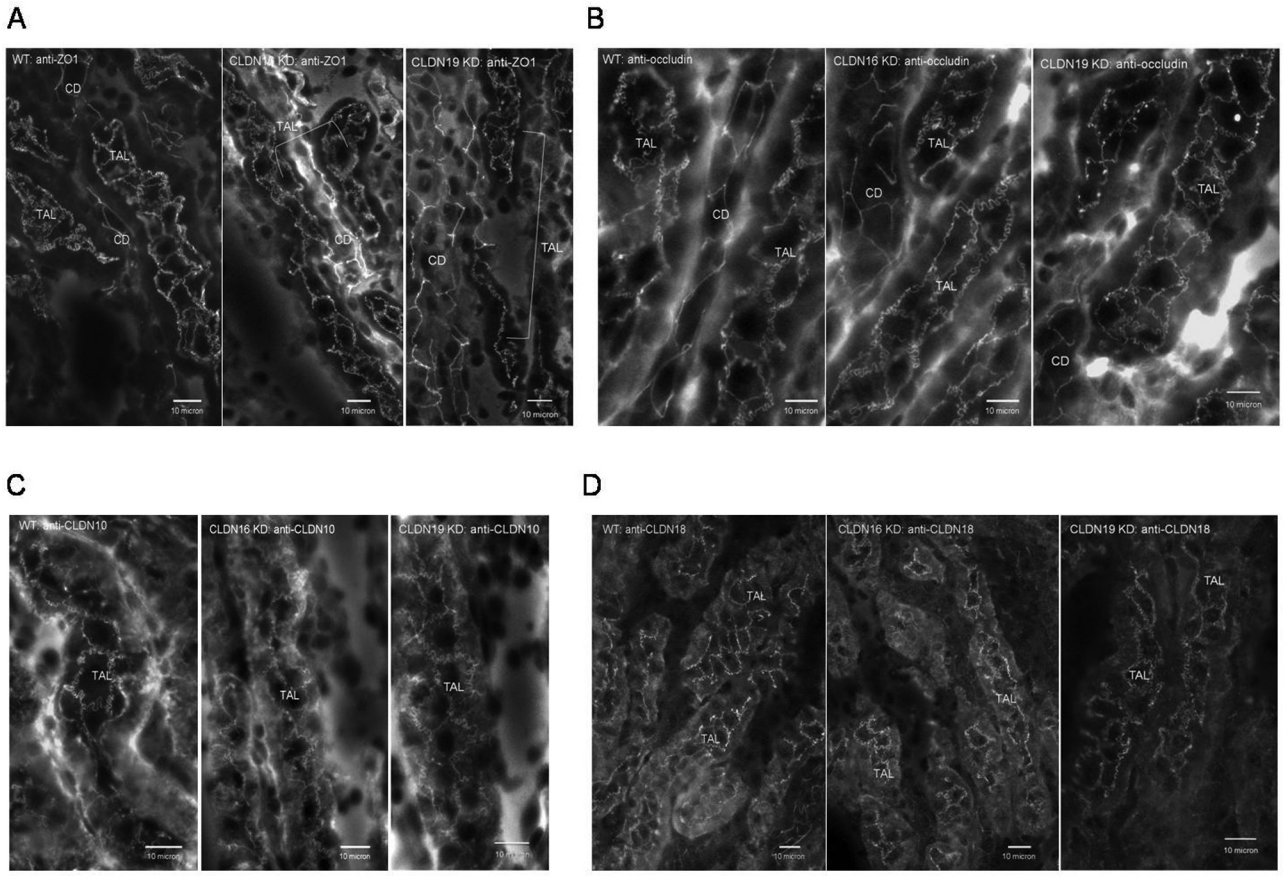

Fig. S9. Immunofluorescence analysis of ZO-1, occludin, CLDN10, and CLDN18 protein localization in the kidney. Cryostat sagittal sections (10 μm) from mouse kidneys show TJ localization of ZO-1 (*A*), occludin (*B*), CLDN10 (*C*), and CLDN18 (*D*) in the TAL of WT and that their localization patterns in the TAL were not affected in CLDN16 KD or CLDN19 KD.

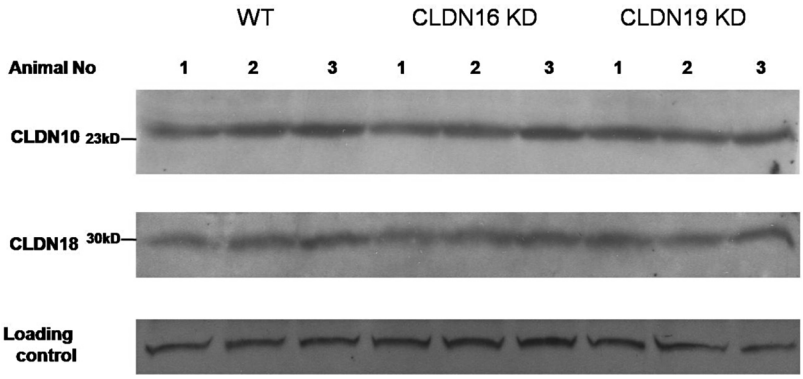

Fig. S10. Analysis of protein levels of CLDN10 and CLDN18 in the kidney. Western immunoblots showing CLDN10 and CLDN18 protein levels in the kidneys of WT, CLDN16 KD and CLDN19 KD mice (N = 3).

Table S1. Abnormalities in Mg^{2+} and Ca^{2+} homeostasis in CLDN19 KD mice

Group	*N*	P_{Mg}, mM	P_{Ca}, mM	$U_{Mg}/U_{Creatinine}$, mg/mg	$U_{Ca}/U_{Creatinine}$, mg/mg
WT	7	0.89 ± 0.03	1.98 ± 0.02	0.718 ± 0.109	0.063 ± 0.019
KD#438	6	0.71 ± 0.03*	2.10 ± 0.05	0.912 ± 0.135	0.375 ± 0.032*
KD#517	6	0.74 ± 0.02*	2.07 ± 0.06	0.864 ± 0.077	0.422 ± 0.051*

Data are mean ± SE. *N*, number of animals; P_{Ca}, P_{Mg}, plasma Ca^{2+} and Mg^{2+} concentrations, respectively; U_{Ca}, U_{Mg}, $U_{Creatinine}$, urinary Ca^{2+}, Mg^{2+}, and creatinine concentrations, respectively. *, Significant difference between WT and KD, $P < 0.05$.

Table S2. Quantitation of gene expression by real-time PCR analyses

Gene	WT	CLDN16 KD	CLDN19 KD
CLDN16	0.1039 ± 0.0157	0.0015 ± 0.0003*	0.0977 ± 0.0130
CLDN19	0.0428 ± 0.0056	0.0403 ± 0.0019	0.00065 ± 0.00005*

Values are presented as ratios relative to the expression level of β-actin (mean ± SE); $N = 3$, the number of animals. *, Significant difference between WT and KD, $P < 0.001$.